

## Effects of Modified Silicon Carbide on The Physical Properties of Bioplastic Blends

Natkrita Prasetsopha and Patcharapon Somdee\*

Department of Materials Engineering, Rajamangala University of Technology Isan, Nakhon Ratchasima, Thailand

Manjunath Shettar

Department of Mechanical and Industrial Engineering, Manipal Institute of Technology, Manipal Academy of Higher Education, Manipal, India

Manauwar Ali Ansari

Institute of Ceramic and Polymer Engineering, University of Miskolc, Miskolc, Hungary

Pranee Chumsamrong

School of Polymer Engineering, Suranaree University of Technology, Nakhon Ratchasima, Thailand

\* Corresponding author. E-mail: patcharaporn.so@rmuti.ac.th

DOI: 10.14416/j.asep.2024.07.015

Received: 19 April 2024; Revised: 7 June 2024; Accepted: 3 July 2024; Published online: 30 July 2024

© 2024 King Mongkut's University of Technology North Bangkok. All Rights Reserved.

### Abstract

The study's goal is to improve the physical properties of biodegradable plastics by mixing poly(lactic acid) (PLA), polybutylene succinate (PBS), and silicon carbide (SiC) to make composites that could be used as filaments for 3D printing. Polymer blends and composites were fabricated using an internal mixer. The fraction of SiC was varied from 10 to 40 phr and filled in PLA/PBS blends with a retained ratio of 80/20 wt.%. Then, the mechanical properties, thermal properties, melt flow rate and morphology of PLA/PBS/SiC composites were investigated. Field emission scanning electron microscope images present a uniform dispersion of silane-treated SiC particles throughout the PLA/PBS matrix. The morphology showed better adhesion between PLA/PBS and treated SiC particles. Therefore, this was also the reason for the improvement of Young's modulus and impact strength when the SiC fraction was increased, which were improved by 33% and 104%, respectively, compared to neat PLA. Furthermore, the melt flow rate increased with an increasing SiC fraction. This might be because adding SiC reduces the viscosity of the composites, which affects the molecular chain movement of the PLA/PBS and the crystallinity of PLA, therefore decreasing the  $\Delta H_m$  of PLA and  $X_{c,PLA}$ . However,  $T_g$  and  $T_m$  of PLA and PBS remained relatively stable with an increasing fraction of SiC particles.

**Keywords:** Mechanical properties, Melt flow rate, Morphology, Poly(lactic acid), Polybutylene succinate, Silicon carbide, Thermal properties

### 1 Introduction

Bioplastics are widely used in many applications, such as packaging, containers, biomedicine, and agriculture [1]–[3]. Poly(lactic acid), or PLA, is an environmentally friendly bioplastic that can decompose. It is often blended with polybutylene succinate (PBS) to improve its disadvantages, such as being brittle and difficult to process. PBS is also a biodegradable plastic. It can be produced from both

natural sources and petroleum bases. Its advantages are high elongation at break, toughness and chemical resistance. PBS is a bioplastic, a friendly material that can be applied to produce biomedical applications [4]–[6]. However, PBS has a higher cost than PLA; therefore, several works have blended PLA with PBS.

PLA/PBS blends are reported to have good properties and compatibility [7]–[11]. However, PLA and PBS have low molecular weight, low melting point, low stiffness and strength, which greatly limits their

potential applications and have no sufficient melt viscosity [12]–[17]. One way to increase the melt viscosity is particle addition because it is a simple and easy method of fabricating composites. Moreover, incorporating particles achieves high melt viscosity due to their influences on shear flow and stress hardening in extensional flow [18]–[22]. Compounding PLA/PBS with inorganic particles can create biopolymer-based composites and give an excellent property with balanced strength and toughness [23]–[27], for example, incorporating clay, calcium carbonate, carbon-based nanoparticles and silicon carbide [28], [29]. Silicon carbide (SiC) is one of the most commonly used materials for reinforcement filler and anti-wear applications. Moreover, SiC has been widely studied because it can be used in several applications, including bearings, bushings, mechanical devices and thermal conductivity devices. However, silane coupling agents can modify the surface of the particles to improve the adhesion between SiC particles and polymer matrix [30].

This work aims to improve the impact strength and stiffness of PLA by blending with PBS and adding SiC as a reinforcement filler to develop the mechanical, thermal and melt flow rate and an eco-friendly material, which is the trend for innovation in materials [31], [32] especially for 3D printing materials [33]–[35]. PLA/PBS ratio i.e., 80/20 wt.% was retained while the fraction of SiC varied of 0, 10, 20, 30 and 40 phr (parts per hundred of resin). Tensile property and impact strength were tested and investigated, while thermal properties were characterized by Differential Scanning Calorimetry (DSC). Furthermore, the melt flow rate was measured and the morphology of PLA/PBS/SiC composites was characterized by field emission scanning electron microscopy (FESEM). Moreover, this study could develop bio-composites from PLA/PBS/SiC. It might be applied to the filament of 3D printing by considering the impact strength, elongation at break and melt flow rate.

## 2 Materials and Methods

### 2.1 Materials

Poly(lactic acid), grade PLA 2003D was purchased from NatureWorks, LLC, Thailand, and polybutylene succinate, grade PBS FZ71PM from PPT MCC Biochem Co., LTD., Thailand. Silicon carbide (SiC) was purchased from Minerals Water, United Kingdom, with around 7  $\mu\text{m}$  (F1200) average particle size. (3-Aminopropyl) triethoxysilane (98%) is a silane

coupling agent that was ordered from Alfa Aesar, China and was used for treating SiC powder in this study.

### 2.2 Sample preparation

The silane coupling and ethanol solution were prepared at 5 wt.% for treating SiC particles before mixing with PLA/PBS blends. In the first step, a mixture of solution containing deionized water and ethanol had a ratio of 25:75 V%/V% and was turned to pH 4–5 by adding acetic acid. Then, (3-Aminopropyl) triethoxysilane was added to reach a 5 wt.% (21 g) concentration. The silane coupling and ethanol solution were mixed by a magnetic stirrer machine for 15 min (Silanized-solution). Then, SiC powder was washed using ultrasonication three times, repeating for 15 min at room temperature. In the final step, the treated SiC powder (Silanized-SiC) was air dried at 90 °C for 24 h and ground to a fine powder before mixing with PLA/PBS (as presented in Figure 1).

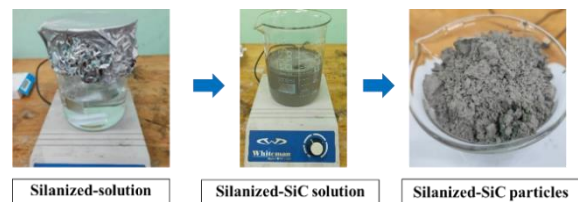


**Figure 1:** Schematic of silanization of SiC particles.

Both PLA and PBS pellets were dried at 50 °C for 48 h using a drying oven. Modified SiC was also dried at 90 °C for 24 h before mixing. All ingredients were mixed using an internal mixer at 200 °C and 50 rpm. The PLA/PBS/SiC formula. PLA/PBS blends with a retained ratio of 80/20 wt.% was prepared and modified SiC was filled between 0 and 40 phr. According to ASTM D638-14 (type V) (2014) and ASTM D256-10 (2010) for tensile and impact testing specimens, five specimens of each combination were produced by hot compression molding at 190 °C for eight minutes for each compound, as illustrated in Figure 2. The dimensions of the tensile specimen are a length overall of 63.5 mm, a length of a narrow section of 9.53 mm, a distance between grips of 25.4 mm, a gage length of 7.62 mm, a width of a narrow section of 3.18 mm, width overall of 9.53 mm and a radius of fillet of 12.7 mm. The dimension of the Izod impact specimen test is length of 63.5 mm, width of 12.7 mm, notch tip radius of 0.25 mm, notch depth of 2.54 mm, notch angle of 45° and thickness of 3 mm.

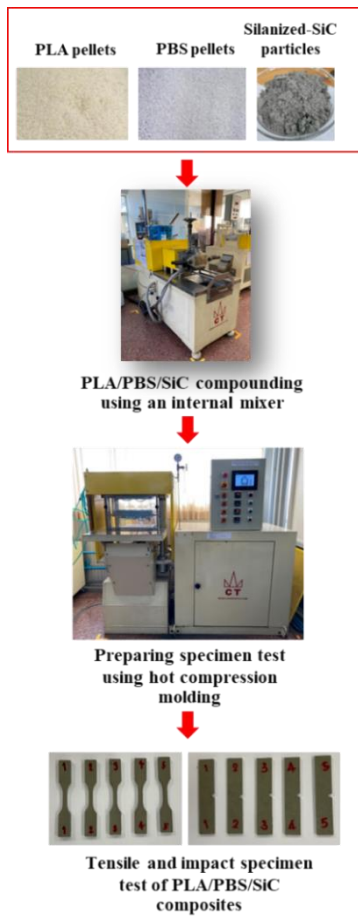


**Figure 2:** Schematic of PLA/PBS/SiC testing specimens preparation.

### 2.3 Testing and characterization

Impact fractured specimens of PLA/PBS/SiC composite were used to investigate the morphology using a field emission scanning electron microscopy technique (FESEM; ZEISS AURIGA). Every sample was coated with gold before the examination. Then, FESEM images of the composites are captured on fractured impact sample surfaces. Moreover, thermal properties were examined by differential scanning calorimeter (Mettler Toledo model DSC1). A first heating scan was used for all samples, starting from 25 to 200 °C at 10 °C/min. After that,  $T_g$ ,  $T_m$ ,  $\Delta H_m$  and  $\%X_c$  were evaluated and presented. Furthermore, a melt flow indexer (GÖTTFERT, mi2.1) was used to measure the melt flow rate (MFR) of all components according to ASTM D1238-13 (2013). The MFR was explored in the unit of g/10 min as the mass (g) of the

sample extruded at the isothermal temperature of 190 °C in 10 min under a constant weight of 2.16 kg through a capillary die.

The tensile test and impact test were investigated by following ASTM D638-14 and ASTM D256-10 at 2.75 J, respectively. A universal testing machine (UTM, Lloyd Instruments, LP10K) was used to test and record the tensile properties. The speed of the crosshead was set at 10 mm/min and tested at 25 °C for all combinations. The impact strength was measured using an impact tester (INSTRON CEAST 9050). All specimens were notched and tested by the Izod method.

## 3 Result and Discussion

### 3.1 Morphology

The fracture surface morphology of PLA/PBS/SiC composites was explored using a field emission scanning electron microscope (FESEM). The impact fractured surface of neat PLA demonstrated a smoother surface than PLA/PBS blends as presented in Figure 3(a). This is due to the poor plastic deformation of neat PLA [36]. Figure 3(b) exhibited the compatibility of the PLA/PBS blends and the homogeneous dispersion of the PBS phase throughout the PLA matrix [37]. The interface area between the PLA and PBS was found as a tiny cavity between the two phases, as observed in Figure 3(c)–(f). It can be indicated as the immiscible blend [38].

The morphology can be seen that SiC particles were embedded within PLA matrix and evenly dispersed throughout PLA/PBS blends matrix as shown in Figure 3(c)–(f) because the surface of SiC particles was treated by silane coupling before mixing. This is due to the surface of modified particles having a granular surface, then becoming rough, and the abundant hydrophobic organic compounds on the surface of silane-treated SiC particles. The modification enhanced the hydrophobicity on the surface of SiC particles [39]. By adding SiC and increasing the SiC fraction into PLA/PBS blends, the fractured surface becomes rougher. FESEM image shows SiC particles embedded into PLA/PBS blend. However, these morphologies show some small cavities as exhibited in Figure 3(c)–(f). These results can support the result of tensile properties and impact strength.

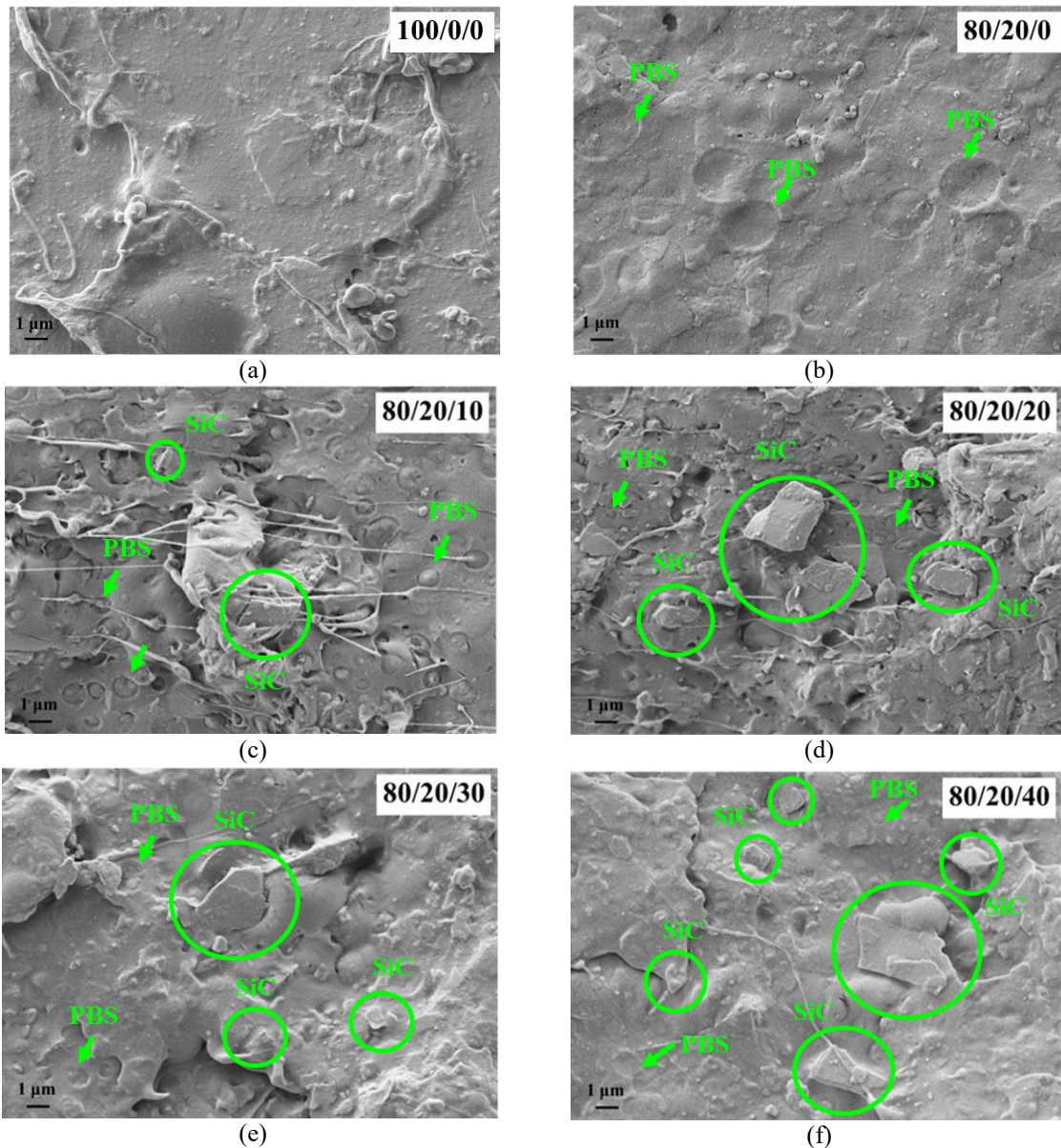


**Figure 3:** FESEM images of PLA/PBS/SiC with PLA/PBS were retained at 80/20 wt.% with different SiC fractions (nominal magnification of 5000x).

### 3.2 Mechanical properties

The tensile stress-strain curve of all samples is presented in Figure 4. All curves presented an initial linear elastic behavior, and after that, a non-linear region until the maximum stress was reached [33]. Neat PLA showed brittle fracture while the blends with PBS of 20 wt.% (80/20/0) showed a notable ductile behavior. When incorporating treated SiC and increasing SiC fraction, the curve becomes like a hard

and brittle material, the strain was decreased, and in contrast, the slope of an initial linear elastic was slightly increased. Furthermore, tensile strength, elongation at break and Young's modulus were obtained from these stress-strain curves. The tensile results consist of tensile strength, elongation at break and Young's modulus of PLA/PBS/SiC composites with varying SiC fractions from 0 to 40 phr were presented in Figures 5–7, respectively.

**Table 1:** Tensile properties and impact strength of PLA/PBS/SiC with PLA/PBS were retained at 80/20 wt.% and different SiC fractions.

PLA/PBS/SiC	Tensile Strength (MPa)	SD	Elongation at Break (%)	SD	Young's Modulus (MPa)	SD	Impact Strength (kJ/m <sup>2</sup> )	SD
100/0/0	50	5	12	1	706	41	2.5	0.1
80/20/0	20	1	70	11	650	45	3.6	0.7
80/20/10	17	1	49	17	687	79	4.7	1.1
80/20/20	22	3	35	12	720	94	5.1	0.5
80/20/30	38	3	15	2	832	65	4.7	0.6
80/20/40	42	2	10	1	939	29	4.7	0.3

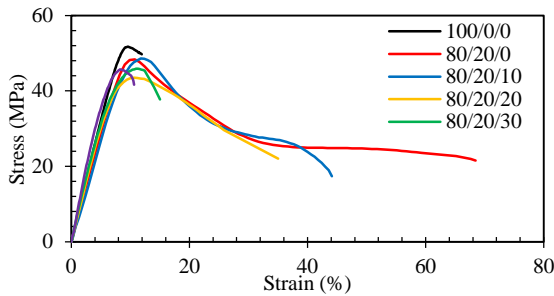


**Figure 4:** Tensile stress-strain curves of PLA/PBS/SiC with PLA/PBS were retained at 80/20 wt.% and different SiC fractions.

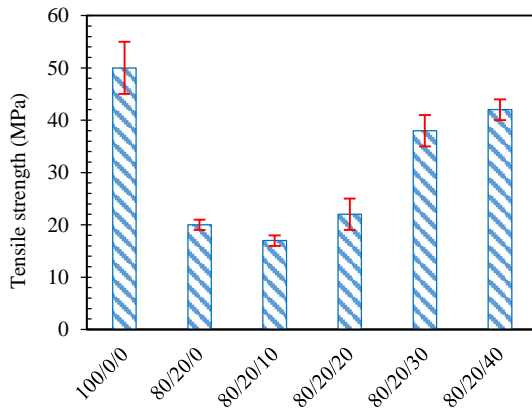


**Figure 5:** Tensile strength of PLA/PBS/SiC with PLA/PBS was retained at 80/20 wt.% and different SiC fractions.

Results show that the tensile strength and percent elongation at the break of neat PLA was 50 MPa and 12%, respectively, while, Young's modulus has a high value of 706 MPa as shown in Table 1. By blending with PBS of 20 wt.%, tensile strength suddenly decreased, but elongation at break suddenly increased. This was because of adding PBS of 20 wt.% which was evenly dispersed into PLA matrix, which led to improvement in the elongation of the blend. At the same time, no compatibility between PLA and PBS decreased tensile strength. As expected, the tensile

strength reduced from 50 to 20 MPa when PBS of 20 wt.% was added. This was because of PBS's lower tensile strength than PLA. Moreover, it was due to its flexibility and toughness of PBS, which improved the elongation at a break of 483% compared to neat PLA, as found that the behavior of the specimen changed from brittle (smooth fractured surface) to ductile (rough fractured surface) fracture [37], [40].

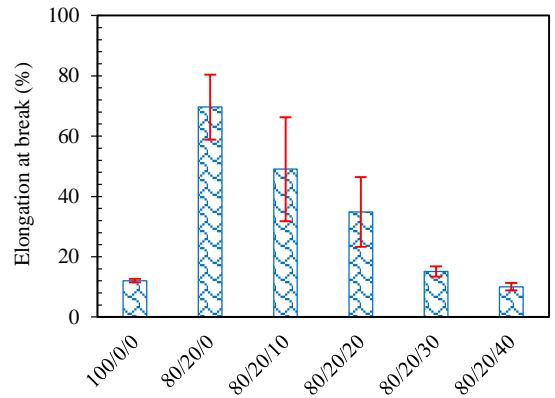


**Figure 6:** Elongation at break of PLA/PBS/SiC with PLA/PBS was retained at 80/20 wt.% and different SiC fractions.

When adding SiC particles, tensile strength tended to increase when increasing SiC fractions as shown in Figure 5 and Table 1. This behavior could be due to good adhesion between treated-SiC particles and PLA/PBS blends [30]. Furthermore, the increasing SiC fraction increases the tensile strength because of the uniform dispersion of SiC particles throughout the PLA/PBS matrix.

In contrast, elongation at break decreased with increasing SiC fractions as shown in Figure 6. This might be due to loading SiC particles, which makes the PLA/PBS matrix lose its flexibility. The insertion of filler is affected by intermolecular force and loose chain entanglement, which decreases the continuous phase of the polymer. Furthermore, the inclusion of SiC particles lowered stress transfer. On the other

hand, the polymer chain relaxation was affected. The cracks were generated during deformation, resulting in a decrease in tensile strength when compared to neat PLA. This is because the concentration of stress at the interface made the polymer chains rigid [41].

Young's modulus of neat PLA was 706 MPa. When blending with 20 wt.% of PBS, Young's modulus slightly decreased to 650 MPa, then, it was enhanced up to 939 MPa by the addition of 40 phr of SiC. It was improved by 33% when compared to neat PLA. Treated-SiC exhibited a notable enhancement in Young's modulus reaching 939 MPa when incorporating 40 phr of SiC as shown in Figure 7. The observed phenomenon resulted from the incorporation of SiC as a ceramic filler resistance to load-induced deformation. This was present due to the high Young's modulus and stiffness exhibited by incorporation and increasing the fraction of SiC [41].

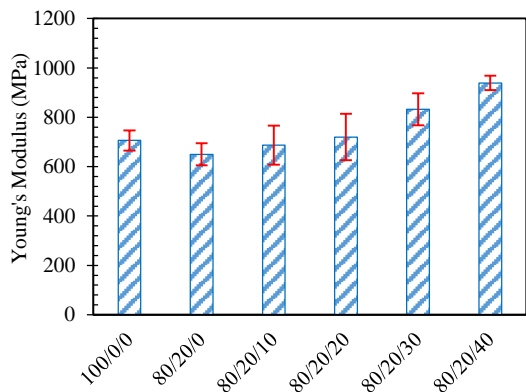


**Figure 7:** Young's modulus of PLA/PBS/SiC with PLA/PBS was retained at 80/20 wt.% and different SiC fractions.

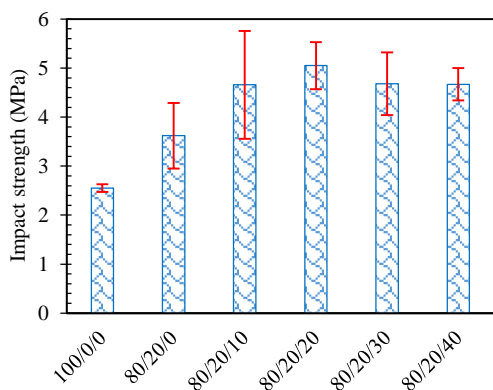


**Figure 8:** Impact strength of PLA/PBS/SiC with PLA/PBS was retained at 80/20 wt.% and different SiC fractions.

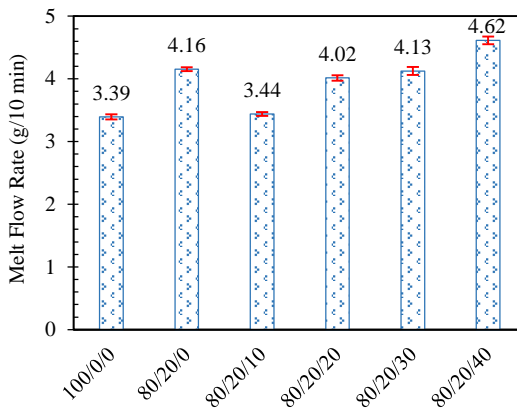


**Figure 9:** Melt flow rate of PLA/PBS/SiC with PLA/PBS was retained at 80/20 wt.% and different SiC fractions.

The impact strength of neat PLA was 2.5 kJ/m<sup>2</sup>. Loading PBS 20 wt.% can enhance the impact strength of polymer blends up to 3.6 kJ/m<sup>2</sup>, because of the flexibility of PBS phase and the even dispersed throughout PLA matrix. When loading SiC particles, uniform distribution of the inorganic fillers in the polymer matrix can improve the force absorption of the polymer composite [42]. The impact strength can be reached at 5.1 kJ/m<sup>2</sup> with a loading of 20 phr of SiC, as shown in Figure 8 and Table 1. It was improved by 104% and 60% compared to neat PLA and PLA/PBS of 80/20 wt.%, respectively. The SiC particles within the PLA/PBS matrix impeded crack propagation by facilitating crack branching, effectively absorbing externally applied energy, and improving impact strength [29]. The other reason was that treating SiC particles with silane coupling can improve the compatibility between PLA/PBS matrix and SiC particles [43]. The impact strength slightly decreased, possibly due to some agglomerating of SiC particles within PLA/PBS matrix when loading a high fraction of SiC (30 and 40 phr).

### 3.3 Melt flow rate

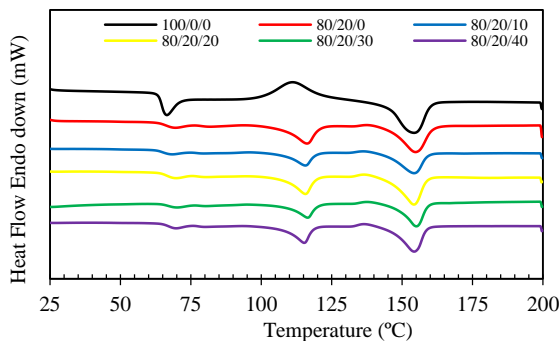
Melt flow rate (MFR) or melt flow index indicates the flowability of the polymer melt and is an indirect indication of the molecular weight and viscosity of the melt. Raising MFR for the blends can be a reason for the decrease in the molecular weight and lack of compatibility of the blend.

Figure 9 presented the MFR of the neat PLA, PLA/PBS blend (80/20 wt.%) and PLA/PBS/SiC composites. By loading with PBS of 20 wt.%, MFR

was raised to 4.16 g/10 min while neat PLA has 3.39 g/10 min. The increase in MFR of the blends might indicate a reduction in the molecular weight of the polymers during melt mixing and immiscibility between PLA and PBS blends. When loading 10 phr of SiC, MFR decreased (3.44 g/10 min), indicating viscosity of the composite was raised. On the other hand, MFR increased with increasing SiC fraction up to 4.62 g/10 min. This might be because SiC particles act as lubricants on the polymer molecule chains. The flat surface of SiC particles can influence the movement of the polymer molecule chains [43]. This also implies that the viscosity of the composites was decreased.

### 3.4 Thermal properties

Thermal properties of neat PLA, PLA/PBS blends and PLA/PBS/SiC composites were examined by DSC thermogram as presented in Figure 10. The DSC thermogram clearly shows the glass transition temperature ( $T_g$ ), crystallization temperature ( $T_c$ ) and melting temperature ( $T_m$ ).



**Figure 10:** DSC thermogram of PLA/PBS/SiC with PLA/PBS was retained of 80/20 wt.% and different SiC fractions.

For neat PLA, the  $T_g$ ,  $T_{c, PLA}$  and  $T_{m, PLA}$  of PLA were 63.5 °C, 111.3 °C and 154.7°C, respectively. For loading PBS of 20 wt.%, DSC thermogram showed  $T_g$ ,  $T_{m, PLA}$  and  $T_{m, PBS}$  were 64.9 °C, 155.0 °C and 116.3 °C, respectively, while  $T_c$  disappeared. This can be indicated that loading PBS does not influence the thermal conductivity of PLA and PBS blends, because of the lack of interaction between PLA and PBS. By loading SiC,  $T_g$ ,  $T_{m, PLA}$  and  $T_{m, PBS}$  in all compositions were nearly the same as those of the PLA/PBS blends (shown in Table 2), indicating that the addition of SiC to PLA/PBS had no effect on both  $T_g$  and  $T_m$  of PLA and PBS. This might indicate the thermodynamics of PLA, PBS and SiC, which are incompatible [44].

However, the area under the endothermic peak of both PLA and PBS decreased with loading more SiC fraction, which reduced the melting enthalpy ( $\Delta H_m$ ) as presented in Table 2. A slight decrease in the melting enthalpy might be related to enhancing the fraction effect of the SiC within the PLA/PBS matrix.

Besides, the incorporation of SiC particles affects the mobility of the PLA and PBS molecular chains and the melting enthalpy is reduced, leading to changes in the crystallinity of both PLA and PBS phases [41]. When blending 20 wt.% of PBS, the degree of crystallinity of PLA ( $X_{c, PLA}$ ) decreased from 50.9 to 28.9%. This indicates that PBS hindered the crystallization rate of PLA [45]. In the case of loading SiC into PLA/PBS, the melting enthalpy was decreased. This might be due to SiC particles hindering the migration and diffusion of both PLA and PBS chains, and constraining the mobility of the molecular chain. This resulted in a reduction of the released melting enthalpy, thereby inducing alterations in the crystalline properties of both PLA and PBS by lowering the degree of crystallinity [41], [46] as exhibited in Table 2.

**Table 2:** Thermal properties of PLA/PBS/SiC with PLA/PBS were retained at 80/20 wt.% and different SiC fractions.

PLA/PBS/SiC	$T_g$ (°C)	$T_{c, PLA}$	$T_{m, PLA}$	$T_{m, PBS}$	$\Delta H_{c, PLA}$	$\Delta H_{m, PLA}$	$\Delta H_{m, PBS}$	$X_{c, PLA}$
100/0/0	63.5	111.3	154.7	N/A	21.7	25.7	N/A	50.9
80/20/0	64.9	N/A	155.0	116.3	N/A	21.5	13.1	28.9
80/20/10	64.3	N/A	154.3	115.8	N/A	20.7	10.8	27.8
80/20/20	65.4	N/A	154.5	115.8	N/A	20.6	11.1	27.7
80/20/30	65.7	N/A	155.2	116.7	N/A	18.9	10.6	25.3
80/20/40	65.9	N/A	154.5	115.3	N/A	19.0	10.1	25.6



#### 4 Conclusions

PLA/PBS/SiC composites were successfully prepared using an internal mixer. FESEM analysis revealed uniform dispersion and good adhesion of modified SiC particles within the PLA/PBS matrix. Preparing PBS and SiC particles in varying fractions significantly influenced the composites' mechanical properties. Young's modulus and impact strength improved with SiC additions ranging from 10 to 40 phr, with Young's modulus reaching 939 MPa at 40 phr and impact strength reaching 5.1 kJ/m<sup>2</sup> at 20 phr. These results indicate that SiC particles enhance the strength and stiffness of PLA/PBS/SiC composites. Additionally, SiC loading increased the MFR by reducing viscosity and enhancing polymer chain mobility during melting. The  $T_g$  and  $T_m$  of PLA and PBS remained largely unaffected by increased SiC content, while  $\Delta H_m$  for both polymers and  $\%X_{c,PLA}$  tended to decrease with higher SiC fractions. This can be attributed to the influence of SiC on the molecular chain motion of PLA and PBS.

#### Acknowledgments

The authors extend our sincere thanks for financial support by 1) Rajamangala University of Technology Isan (RMUTI) (Fundamental Fund 2023), 2) Thailand Science Research and Innovation (TSRI), and 3) National Science, Research and Innovation Fund (NSRF), Project no. 181818.

#### Author Contributions

N.P., P.S., M.S., and P.C.: carried out the experiments; P.S., N.P., M.S., and M.A.A.: coordinated the project; N.P., M.S., P.C., M.A.A., and P.S.: analyzed the data and wrote the manuscript; P.S., N.P., and M.A.A.: prepared the graphs. All authors have read and agreed to the published version of the manuscript.

#### Conflicts of Interest

The authors declare no conflict of interest.

#### References

- [1] M. Y. Mollajavadi, F. F. Tarigheh, and R. Eslami-Farsani, "Self-healing polymers containing nanomaterials for biomedical engineering applications: A review," *Polymer Composites*, vol. 44, no. 10, pp. 6869–6889, 2023, doi: 10.1002/pc.27603.
- [2] D. Jubinville, J. Sharifi, H. Fayazfar, and T. H. Mekonnen, "Hemp hurd filled PLA-PBAT blend biocomposites compatible with additive manufacturing processes: Fabrication, rheology, and material property investigations," *Polymer Composites*, vol. 44, no. 12, pp. 8946–8961, 2023, doi: 10.1002/pc.27749.
- [3] B. Leonard, R. Anamarija, I. Marica, and I. Hrvoje, "Medical-grade poly(lactic acid)/hydroxyapatite composite films: thermal and In Vitro degradation properties," *Polymers*, vol. 15, no. 15, pp. 1–16, 2023, doi: 10.3390/polym15061512.
- [4] M. Gigli, M. Fabbri, N. Lotti, R. Gamberini, B. Rimini, and A. Munari, "Poly(butylene succinate)-based polyesters for biomedical applications: A review," *European Polymer Journal*, vol. 75, pp. 431–460, 2016, doi: 10.1016/j.eurpolymj.2016.01.016.
- [5] S. Wang and Q. Xing, "Study on properties and biocompatibility of poly(butylene succinate) and sodium alginate biodegradable composites for biomedical applications," *Materials Research Express*, vol. 9, pp. 1–14, 2022, doi: 10.1088/2053-1591/ac896f.
- [6] L. Aliotta, M. Seggiani, A. Lazzeri, V. Gigante, and P.A. Cinelli, "A brief review of poly(butylene succinate) (PBS) and its main copolymers: Synthesis, blends, composites, biodegradability, and applications," *Polymers*, vol. 14, p. 844, 2022, doi: 10.3390/polym14040844.
- [7] S. Shen, K. Rodion, T. Sengul, and K. Stephan, "Polylactide (PLA) and its blends with poly(butylene succinate) (PBS): A brief review," *Polymers*, vol. 11, no. 7, p. 1193, 2019, doi: 10.3390/polym11071193.
- [8] Y. Deng and N. L. Thomas, "Blending poly(butylene succinate) with poly(lactic acid) ductility and phase inversion effects," *European Polymer Journal*, vol. 71, pp. 534–546, 2015, doi: 10.1016/j.eurpolymj.2015.08.029.
- [9] X. Zhao, D. Zhang, S. Yu, H. Zhou, and S. Peng, "Recent advances in compatibility and toughness of poly(lactic acid)/poly(butylene succinate) blends," *e-Polymers*, vol. 21, pp. 793–810, May 2021, doi: 10.1515/epoly-2021-0072.
- [10] T. Y. Qiu, M. Song, and L. G. Zhao, "Testing, characterization and modelling of mechanical behaviour of poly(lactic acid) and poly(butylene succinate) blends," *Mechanics of Advanced*



- Materials and Modern Processes*, vol. 2, no. 7, pp. 1–11, 2016, doi: 10.1186/s40759-016-0014-9.
- [11] T. Yokohara and M. Yamaguchi, “Structure and properties for biomass-based polyester blends of PLA and PBS,” *European Polymer Journal*, vol. 44, pp. 677–685, 2008, doi: 10.1016/j.eurpolymj.2008.01.008.
- [12] R. Wang, S. Wang, Y. Zhang, C. Wan, and P. Ma, “Toughening modification of PLLA/PBS blends via in situ compatibilization,” *Polymer Engineering and Science*, 2009, doi: 10.1002/pen.21210.
- [13] S. A. Rafiqah, A. Khalina, A. S. Harmaen, I. A. Tawakkal, K. Zaman, M. Asim, M. N. Nurrazi, and C. H. Lee, “A review on properties and application of bio-based poly(butylene succinate),” *Polymers*, vol. 13, p. 1436, 2021, doi: 10.3390/polym13091436.
- [14] V. Ojijo, S. S. Ray, and R. Sadiku, “Role of specific interfacial area in controlling properties of immiscible blends of biodegradable polylactide and poly [(butylene succinate)-co-adipate],” *ACS Applied Materials & Interfaces*, vol. 4, pp. 6690–6701, 2012, doi: 10.1021/am301842e.
- [15] V. Ojijo, S. S. Ray, and R. Sadiku, “Toughening of biodegradable polylactide/poly(butylene succinate co-adipate) blends via in situ reactive compatibilization,” *ACS Applied Materials & Interfaces*, vol. 5, pp. 4266–4276, 2013, doi: 10.1021/am400482f.
- [16] B. Palai, S. Mohanty, and S. K. Nayak, “Synergistic effect of polylactic acid (PLA) and poly(butylene succinate-co-adipate) (PBSA) based sustainable, reactive, super toughened eco-composite blown films for flexible packaging applications,” *Polymer Testing*, vol. 83, Mar. 2020, Art. no. 106130, doi: 10.1016/j.polymertesting.2019.106130.
- [17] H. Eslami and M. R. Kamal, “Elongational rheology of biodegradable poly(lactic acid)/poly[(butylene succinate)-co-adipate] binary blends and poly(lactic acid)/Poly[(butylene succinate)-co-adipate]/clay ternary nanocomposites,” *Journal of Applied Polymer Science*, 2012, doi: 10.1002/APP.37928.
- [18] M. Keramati, I. Ghasemi, M. Karrabi, and H. Azizi, “Microcellular foaming of PP/EPDM/organoclay nanocomposites: The effect of the distribution of nanoclay on foam morphology,” *Polymer Journal*, vol. 44, pp. 433–438, Feb. 2012, doi: 10.1038/pj.2012.2.
- [19] T. Yokohara, K. Okamoto, and M. Yamaguchi, “Effect of the shape of dispersed particles on the thermal and mechanical properties of biomass polymer blends composed of poly(L-lactide) and poly(butylene succinate),” *Journal of Applied Polymer Science*, vol. 117, no. 4, pp. 2226–2232, Aug. 2010, doi:10.1002/app.31959.
- [20] I. S. Choi, Y. K. Kim, S. H. Hong, H.-J. Seo, S.-H. Hwang, J. Kim, and S. K. Lim, “Effects of polybutylene succinate content on the rheological properties of polylactic acid/polybutylene succinate blends and the characteristics of their fibers,” *Materials*, vol. 17, 662, Jan. 2024, doi: 10.3390/ma17030662.
- [21] Monika, A. K. Pal, S. M. Bhasney, P. Bhagabati, and V. Katiyar, “Effect of dicumyl peroxide on a poly (lactic acid) (PLA) / poly(butylene succinate) (PBS) / functionalized chitosan-based nanobio - composite for packaging: A reactive extrusion study,” *ACS Omega*, vol. 3, pp. 13298–13312, 2018, doi: 10.1021/acsomega8b00907.
- [22] J. Zhou, Z. Yao, C. Zhou, D. Wei, and S. Li, “Mechanical properties of PLA/PBS foamed composites reinforced by organophilic montmorillonite,” *Journal of Applied Polymer Science*, 2014, Art. no. 40773, doi: 10.1002/app.40773.
- [23] S. Coiai, S. Javarone, F. Cicogna, W. Oberhause, M. Onor, A. Pucci, P. Minei, G. Iasilli, and E. Passaglia, “Fluorescent LDPE and PLA nanocomposites containing fluorescein-modified layered double hydroxides and their ON/OFF responsive behavior towards humidity,” *European Polymer Journal*, vol. 99, pp. 189–201, Dec. 2017, doi: 10.1016/j.eurpolymj.2017.12.02.
- [24] F. Iñiguez-Franco, R. Auras, M. Rubino, K. Dolan, H. Soto-Valdez, and S. Selke, “Effect of nanoparticles on the hydrolytic degradation of PLA-nanocomposites by water-ethanol solutions,” *Polymer Degradation and Stability*, vol. 146, pp. 287–297, Nov. 2017, doi: 10.1016/j.polymdegradstab.2017.11.004.
- [25] H. Wu, S. Nagarajan, J. Shu, T. Zhang, L. Zhou, Y. Duan, and J. Zhang, “Green and facile surface modification of cellulose nanocrystal as the route to produce poly(lactic acid) nanocomposites with improved properties,” *Carbohydrate Polymers*, vol. 197, pp. 204–214, May 2018, doi:10.1016/j.carbpol.2018.05.087.
- [26] C. Liu, S. Ye, and J. Feng, “Promoting the dispersion of graphene and crystallization of



- poly (lactic acid) with a freezing-dried graphene/PEG masterbatch,” *Composites Science and Technology*, vol. 144, pp. 215–222, Mar. 2017, doi: 10.1016/j.compscitech.2017.03.031.
- [27] R. Avolio, R. Castaldo, M. Avella, M. Cocca, G. Gentile, S. Fiori, and E. E. Maria, “PLA-based plasticized nanocomposites: Effect of polymer/plasticizer/filler interactions on the time evolution of properties,” *Composites Part B Engineering*, vol. 152, pp. 267–274, Jul. 2018, doi: 10.1016/j.compositesb.2018.07.011.
- [28] X. Zhang, B. Geng, H. Chen, Y. Chen, Y. Wang, L. Zhang, H. Liu, H. Yang, and J. Chen, “Extraordinary toughness enhancement of poly(lactic acid) by incorporating very low loadings of noncovalent functionalized graphene-oxide via masterbatch-based melt blending,” *Chemical Engineering Journal*, vol. 334, pp. 2014–2020, Feb. 2018, doi: 10.1016/j.cej.2017.11.102.
- [29] J. B. Zhang, Z. Heng, F. L. Jin, and S. J. Park, “Enhancement of impact strength of poly(lactic acid)/silicon carbide nanocomposites through surface modification with titanate-coupling agents,” *Bulletin of Materials Science*, vol. 43, no. 6, Dec. 2019, doi: 10.1007/s12034-019-1977-z.
- [30] J. Abenojar, J. C. del Real, M. A. Martinez, and M. C. de Santayana, “Effect of silane treatment on SiC particles used as reinforcement in epoxy resins,” *The Journal of Adhesion*, vol. 85, no.6, pp. 287–301, 2009, doi: 10.1080/00218460902880131.
- [31] S. K. Palaniappan, M. K. Singh, S. M. Rangappa, and S. Siengchin, “Eco-friendly biocomposites: A step towards achieving sustainable development goals,” *Applied Science and Engineering Progress*, vol. 17, no. 4, 2024, Art. no. 7373, doi: 10.14416/j.asep.2024.02.003.
- [32] I. Suyambulingam, S. M. Rangappa, and S. Siengchin, “Advanced materials and technologies for engineering applications,” *Applied Science and Engineering Progress*, vol. 16, no. 3, 2023, Art. no. 6760, doi: 10.14416/j.asep.2023.01.008.
- [33] E. M. Agaliotis, B. D. Ake-Concha, A. May-Pat, J. P. Morales-Arias, C. Bernal, A. Valadez-Gonzalez, P. J. Herrera-Franco, G. Proust, J. F. Koh-Dzul, J. G. Carrillo, and E. A. Flores-Johnson, “Tensile behavior of 3D printed polylactic acid (PLA) based composites reinforced with natural fiber,” *Polymers*, vol. 14, no. 19, 2022, Art. no. 3976, doi: 10.3390/polym14193976.
- [34] V. Raghunathan, V. Ayyappan, S. M. Rangappa, and S. Siengchin, “Development of fiber-reinforced polylactic acid filaments using untreated/silane-treated *trichosanthes cucurbitina* fibers for additive manufacturing,” *Journal of Elastomers & Plastics*, vol. 56, no. 3, pp. 277–292, 2024, doi: 10.1177/00952443241229186.
- [35] A. Vinod, J. Tengsuthiwat, R. Vijay, M. R. Sanja, and S. Siengchin, “Advancing additive manufacturing: 3D-printing of hybrid natural fiber sandwich (Nona/Soy-PLA) composites through filament extrusion and its effect on thermomechanical properties,” *Polymer Composites*, pp. 1–23, 2024, doi: 10.1002/pc.28302.
- [36] L. Jiang, J. Zhang, and M. P. Wolcott, “Comparison of polylactide/nano-sized calcium carbonate and polylactide/montmorillonite composites: Reinforcing effects and toughening mechanisms,” *Polymer*, vol. 48, no. 26, pp. 7632–7644, Dec. 2007, doi: 10.1016/j.polymer.2007.11.001.
- [37] E. A. Hassan, S. E. Elarabi, Y. Wei, and M. Yu, “Biodegradable poly (lactic acid)/poly (butylene succinate) fibers with high elongation for health care products,” *Textile Research Journal*, vol. 88, no. 15, pp. 1735–1744, 2018, doi: 10.1177/0040517517708538.
- [38] M. Shibata, Y. Inoue, and M. Miyoshi, “Mechanical properties, morphology, and crystallization behavior of blends of poly(l-lactide) with poly (butylene succinate-co-l-lactate) and poly (butylene succinate),” *Polymer*, vol. 47, pp. 3557–3564, May 2006, doi: 10.1016/j.polymer.2006.03.065.
- [39] X. Shang, Y. Zhu, and Z. Li, “Surface modification of silicon carbide with silane coupling agent and hexadecyl iodide,” *Applied Surface Science*, vol. 394, pp. 169–177, Oct. 2016, doi: 10.1016/j.apsusc.2016.10.102.
- [40] H. Elwathig, W. You, J. He, and M. Yu, “Dynamic mechanical properties and thermal stability of poly (lactic acid) and poly (butylene succinate) blends composites,” *Journal of Fiber Bioengineering and Informatics*, vol. 6, no. 1, pp. 85–94, 2013, doi: 10.3993/jfbi03201308.
- [41] Z. C. Lule, E. W. Shiferaw, and J. Kim, “Thermomechanical properties of SiC-filled polybutylene succinate composite fabricated via melt extrusion,” *Polymers*, vol. 12, 2020, Art. no. 418, doi: 10.3390/polym12020418.

- [42] W. Pivsa-Art and S. Pivsa-Art, "Effect of talc on mechanical characteristics and fracture toughness of poly(lactic acid)/poly(butylene succinate) blend," *Journal of Polymers and the Environment*, vol. 27, pp. 1821–1827, 2019, doi: 10.1007/s10924-019-01478-z.
- [43] S. S. Yao, Q. Q. Pang, R. Song, F. L. Jin, and S. J. Park, "Fracture toughness improvement of poly(lactic acid) with silicon carbide whiskers," *Macromolecular Research*, vol. 24, no. 11, pp. 961–964, 2016, doi: 10.1007/s13233-016-4144-z.
- [44] P. Chaiwutthinan, S. Chuayjuljit, S. Srasomsub, and A. Boonmahitthisud, "Composites of poly(lactic acid)/poly(butylene adipate-co-terephthalate) blend with wood fiber and wollastonite: Physical properties, morphology, and biodegradability," *Journal of Applied Polymer Science*, vol. 136, no. 21, Jan. 2019, Art. no. 47543, doi: 10.1002/app.47543.
- [45] D. Ji, Z. Liu, X. Lan, F. Wu, B. Xie, and M. Yang, "Morphology, rheology, crystallization behavior, and mechanical properties of poly(lactic acid)/poly(butylene succinate)/dicumyl peroxide reactive blends," *Journal of Applied Polymer Science*, vol. 131, no. 3, Sep. 2013, Art. no. 39580, doi: 10.1002/app.39580.
- [46] Y. Guo, S. Zhu, Y. Chen, and D. Li, "Thermal properties of wood-plastic composites with different compositions," *Materials*, vol. 12, no. 6, 2019, Art. no. 881, doi: 10.3390/ma12060881.